

## Seismic Response of Isolated Buildings with Adding SMA-Based Recentering Damping Devices and Rotation Friction Dampers

Alaa Barmo<sup>(1)</sup>  
Dr. Hala Tawfek Hasan<sup>(2)</sup>      Dr. Mayada Al-Ahmad Al- Kousa<sup>(3)</sup>

### ABSTRACT

The effect of ground motions in building might be decreased by adding the seismic isolation system.

In buildings that are isolated by this system of isolation, it should be getting back to their initial place by controlling the deformations and displacements especially peak deformations and it should have the possibility to restore the deformations.

Civil engineering has lots of smart materials that may handle this case optimally and behave very well in a range of engineering applications, like shape memory alloy (SMA). These materials have several properties such as superelastic characteristics and the effects of shape memory.

This paper compares the effectiveness of the friction-viscoelastic dampers (FD) with that of the recentering SMAs by conducting Nonlinear Time History analysis to an isolated reinforced concrete building with different three heights (eight, twelve, and sixteen stories), considering two cases: the first case is base isolation system (lead Rubber Bearings LRB+ Flat Sliding Bearing FSB) with additional Rotation Fiction Damper FD, and the second case is base isolation system (LRB+FSB) with additional Re-SMAs. The periods, displacements, and shear forces distribution considering different building height for each system are compared.

The results show a significant improvement in the building performance by using recentering (SMAs) with isolation system in terms of reducing Displacements (on average 7%) and Drift (on average 16%) compared to the use of FD, with increasing building's heights, it restored successfully the building to the original place after the ground motion. Also, using the characteristics of the recentering damping devices SMAs is efficient for decreasing displacement and lateral deformation in the level of the isolator, and this will help in reserving isolation efficacy and protecting the superstructure when increasing the elasticity of the structure.

**Keywords:** Seismic isolation, Shape memory alloys, Super elasticity, Friction- dampers, Smart Material, Recentering, Residual displacement, Drift

---

<sup>(1)</sup> Candidate doctoral in the Structural Earthquake Engineering Department - Higher Institute of Earthquake Studies & Research, University of Damascus, Damascus, Syria. [engalaabarmo@yahoo.com](mailto:engalaabarmo@yahoo.com)

<sup>(2)</sup> Professor in the Structural Earthquake Engineering Department - Higher Institute of Earthquake Studies & Research, University of Damascus, Damascus, Syria. [hala.hasan@damascusuniversity.edu.sy](mailto:hala.hasan@damascusuniversity.edu.sy)

<sup>(3)</sup> Professor at Structural Engineering Department-civil engineering- University of Damascus, Damascus, Syria. [maykousa@hotmail.com](mailto:maykousa@hotmail.com)

## الاستجابة الزلزالية للمباني المعزولة مع إضافة أجهزة التخميد وإعادة التمرکز من خلائط ذاكرة الشكل SMAs ومخمدات الاحتكاك الدوراني FD

م. علاء برمود<sup>(1)</sup>

د. م. هاله توفيق حسن<sup>(2)</sup> د. م. ميادة الأحمد الكوسا<sup>(3)</sup>

### الملخص

يمكن تخفيض انتقال حركة الأرض الناتجة عن الزلازل إلى المنشآت عن طريق إضافة أنظمة العزل الزلزالية لها، ويجب أن تكون أجهزة العزل المستخدمة في المباني المعزولة زلزالياً قادرة على التحكم بالتشوهات والانتقالات وخاصة العظمة ولها قدرة كافية على إعادة المنشأ إلى موقعه الأساسي بعد حدوث الزلازل. يوجد في الهندسة المدنية الكثير من المواد الذكية التي يمكن استخدامها في العديد من مجالات التطبيقات الهندسية. تعتبر خلائط ذاكرة الشكل (SMA) من أهم هذه المواد حيث تملك العديد من الخصائص المميزة مثل المرونة الفائقة وتأثيرات ذاكرة الشكل.

في هذا البحث تم مقارنة فعالية استخدام مخمدات الاحتكاك الدوراني (FD) مع فعالية استخدام مخمدات خلائط ذاكرة الشكل (Re-SMA) كأجهزة تخميد وإعادة تمرکز عن طريق إجراء التحليل الديناميكي للاخطي للسجل الزمني لمبنى خرساني معزول عند القاعدة مع ارتفاعات مختلفة (ثمانية، اثنا عشر، ستة عشر طابقاً)، وأخذ بعين الاعتبار حالات الدراسة: الأولى استخدام نظام العزل الأساسي (العوازل المطاطية LRB مع الصفائح الاحتكاكية FSB) بإضافة مخمدات الاحتكاك الدوراني (FD)، والثانية باستخدام نظام العزل الأساسي (LRB مع FSB) بإضافة مخمدات خلائط ذاكرة الشكل (Re-SMA)، وإجراء المقارنات مع المبنى بأساسات تقليدية من حيث (الدور، الانتقالات، الإزاحات الطابقية، قوة القص القاعدي) وأخذ بعين الاعتبار ارتفاع المبنى لكل نظام عزل. وأظهرت النتائج الفعالية الكبيرة لاستخدام أسلاك خلائط ذاكرة الشكل (SMAs) كأجهزة تخميد وإعادة تمرکز مع نظام العزل الأساسي (LRB مع FSB) في تحسين أداء المبنى فوق نظام العزل من تخفيض الانتقالات (بمعدل 7%) والإزاحات المتبقية (بمعدل 16%) مقارنة مع استخدام مخمدات الاحتكاك (FD) وإعادة المنشأ لمكانه الأساسي بعد حدوث الزلازل وذلك لحالات ارتفاع المنشأ (ثمانية، اثنا عشر، ستة عشر طابقاً). كما أن استخدام مخمدات إعادة التمرکز Re-SMA مفيد للتحكم في الانتقالات والإزاحات المتبقية على مستوى طابق العزل، والذي سيساعد في الحفاظ على كفاءة نظام العزل وحماية المنشأ عند زيادة مرونته.

الكلمات المفتاحية: العزل الزلزالي، خلائط ذاكرة الشكل (SMAs)، المرونة الفائقة، المخمدات الاحتكاكية، المواد الذكية، إعادة التمرکز، الانتقالات المتبقية، الإزاحات الطابقية.

<sup>(1)</sup> طالب دكتوراه في قسم الهندسة الإنشائية الزلزالية - المعهد العالي للبحوث والدراسات الزلزالية، جامعة دمشق، دمشق، سوريا. [engalaabarmo@yahoo.com](mailto:engalaabarmo@yahoo.com)

<sup>(2)</sup> أستاذ في قسم الهندسة الإنشائية الزلزالية - المعهد العالي للبحوث والدراسات الزلزالية، جامعة دمشق، دمشق، سوريا. [hala.hasan@damascusuniversity.edu.sy](mailto:hala.hasan@damascusuniversity.edu.sy)

<sup>(3)</sup> أستاذ في قسم الهندسة الإنشائية - الهندسة المدنية - جامعة دمشق، دمشق، سوريا. [maykousa@hotmail.com](mailto:maykousa@hotmail.com)

## 1. INTRODUCTION

Designing the Seismic isolators is always done with a small horizontal stiffness, but a balance must be achieved in practical isolation systems between the extent of force limitation and the acceptable relative displacements across the isolation system during earthquakes, [17]. Therefore, the use of the seismic isolation system in structures has a major positive role for buildings which are resistant to earthquakes [3].

According to the principle of structural dynamics, seismic isolators are required to have much smaller lateral stiffness than that of the protected superstructure. Although adding stiffness or damping at the isolation level is not suggested from the viewpoint of protecting the superstructure [18], small stiffness and damping may result in excessive deformation at the isolation level towards the earthquake attack direction.

In practical applications, the allowable deformation space for isolation system is usually limited by the adjacent structures or foundations. In fact, as reported in the Northridge earthquake [19], Increasing the period and the flexibility to isolated structures consider the most important features of seismic isolation systems that leads to the exclusion risk of the phenomenon of tinnitus, additional to rises the drift ratio. [11], and this drift can be reduced by increasing damping through the addition of seismic dampers of structure with seismic isolators [5],[20],[21]. SMA is one example of smart materials that exhibit several unique characteristics such as shape memory effect, super-elasticity, and energy dissipation features. Due to these characteristics, Shape Memory Alloys

have widely attracted attention in passive control of structures in recent years [20].

In a series of publications that studied the effectiveness of SMA materials for use in seismic applications, they also studied the implementation of various states of SMA materials for the use of special dampers in structures. They proposed different recentering or dissipating devices based on experimental results. Ma and Cho [21] presented a re-centering SMA damping devices which consists of two groups of SMA wires and two springs, functioning as energy dissipating and re-centering groups, respectively, the studies of using SMA damping devices in the base isolation system of buildings are getting increasing attention. For example, Ponzo et al [22], compared three different isolation systems through shaking table tests and found that the SMA damping devices is better than the counterparts.

## 2. RESEARCH SIGNIFICANCE

The significance of this paper springs out of studying the efficiency of shape memory alloy (SMA) damping devices to raise the efficiency of frictional seismic isolation systems for structures by adding a re-centering force to seismic isolation and reducing the remaining displacement for them, thus ensuring the sustainability of their effectiveness through the superelastic behavior of shape memory alloy (SMA), especially on tensile.

## 3. RESEARCH OBJECTIVE:

Studying the effectiveness of using recentering shape memory alloys Damping Devices (SMAs) in base isolation system of multi-story isolated structure, and comparing them with

using rotational friction dampers (FD) with the base isolation system.

#### 4. RESEARCH METHODOLOGY:

- A summary and review of previous researches.
  - A theoretical overview and modeling to isolation and damping devices (LRB+FSB), (FD, SMAs) used in the research.
  - Analytical study using the SAP2000-V22 program and results:
- Modeling and studying the isolation concrete building **Figure (2)** with the same specifications of the reference study as Tracy [11], (with different three heights (8, 12, and 16 stories, by using El-Centro earthquake **Figure (1)** for the nonlinear time history analysis with considering two cases:
- 1- Base Isolation system (LRB+FSB) with FD.
  - 2- Base isolation system (LRB+FSB) with Rc-SMAs.
- Results

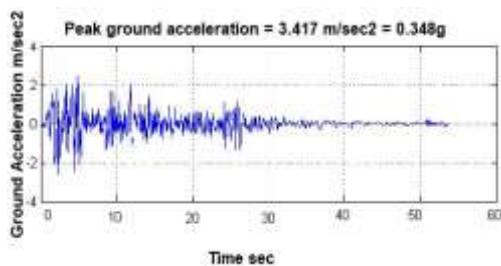


Figure (1): Shows El Centro Earthquake Waves

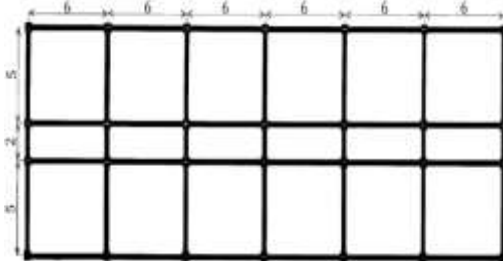


Figure (2): plan of the studied building

## 5. TYPES OF SEISMIC ISOLATION BEARINGS AND RECENTERING DAMPERS: [1],[2]

The quality of the bearings used in any seismic isolation system structure is the reason of its success, which is supposed to provide horizontal flexibility and damping required in addition to the Re-centering force.

### 5.1. TYPES OF SEISMIC ISOLATION BEARINGS:

There are two categories of modern seismic isolation systems for the base:

#### 1) Electrometric bearing system:

One of the most important rubber bearings used in isolation structures is low or high damping rubber bearings or low damping natural rubber with lead core (LRB).

#### 2) Sliding Bearing systems:

Based system for energy dissipation on the friction generated between the composite material which usually consists of high-strength oily or gummy materials known as "PTFE" (Poly tetra fluoro ethylene), and sliding surfaces of steel (stainless steel).

### 5.2. SEISMIC DAMPERS AND RECENTERING DAMPERS: [5]

The seismic isolation devices are usually manufactured typically to dissipate the energy and to control the maximum movement of the isolation device. In spite of this, we still need the complementary mechanisms of the insulation system (dampers) to dissipate energy, recentering isolation devices and

to reduce the displacements. Here are some types of dampers:

### 5.2.1. ROTATION FRICTION DAMPERS (FD): [5]

This device as shown in **Figure 3 (a, b)**, is designed to dissipate seismic energy and protect buildings from structural damage during moderate and severe earthquakes.

Rotational friction damper (FD) is also used with other insulation systems such as (LRB) or (FPS) and others, as complementary dampers to control the Isolation deformation, and for the formation of a hybrid isolation systems.

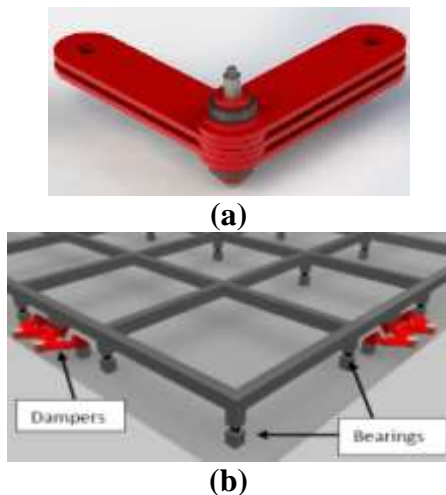


**Figure 3): (a) damper (FD) and (b) its place in the construction within isolation system.**

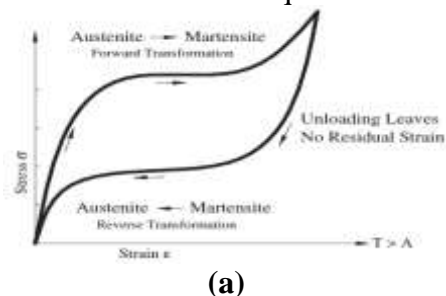
### 5.2.2. Shape memory alloys:

SMA's are a class of metal materials, which have excellent super-elasticity when the environmental temperature is above the phase transformation threshold [23]. This feature is attributed to the solid-to-solid transformation between two crystallographic phases, namely, austenite and martensite, which makes SMA's able

to undergo large strains (8% - 10%) without leaving permanent deformations in the material. They can recover their initial shape at the end of the deformation process, instinctively (called super-elasticity) or by heating (called shape memory effect) as shown in **Figure (4)**.

The most appropriate characteristic of SMA's which is used in passive control of structures is superelastic behavior in which the material can recover large deformations of order of 8 percent while producing flag-shaped hysteresis.

The second feature of the SMA is the shape memory effect. When the material is in Martensite form, the application of stress leads to the twinning of Martensite. The detwinning process begins by removal of stress and some residual strain will be remained at zero stress, that can be recovered by heating the material above a specific temperature. Other desirable characteristics of SMA's are high energy dissipation capacity, stability of hysteresis loop, and high fatigue resistance. Added to all those characteristics, the relatively high stiffness and strength make SMA a promising material for control of structures in severe earthquakes.





(b)  
**Figure (4): Stress-strain curves for SMAs: (a) super-elasticity effect; (b) shape memory effect. [23]**

Because most civil engineering applications of SMA are related to the use of bars and wires, a one-dimensional phenomenological model is often considered suitable due to several merits, including large re-centering strain, good energy dissipation, high fatigue life, and outstanding corrosion resistance, Nitinol/FNCATB SMA is widely used in current seismic application research [24].

The superelastic behavior of the Nitinol/FNCATB wires can only be achieved beyond a certain temperature range. A decrease in temperature is equivalent to an increase in stress for the SMA. Consequently, with decreasing the value of the ambient temperature, a lower level of stress triggers the phase transformation. The beneficial aspect of the super-elasticity can only be attained at elevated temperatures, at which the Austenite phase is stable.

These are important considerations for designer because the operating temperature needs to be reasonably high to retain such effect.

The temperature range between which the super-elasticity can be made use of are (0–40) degrees for Nitinol. For the FNCATB, the lower temperature range is as low as (– 62) degree and the higher one is much above the ambient temperature.

These ranges show that the working temperature range for FNCATB is of much higher magnitude than the Nitinol [24]. So, FNCATB SMA wire is selected to fabricate the Re-centering Damping Devices. Many researchers have proposed uniaxial models for SMA. **Figure (5)** shows the 1D super-elastic model of SMA material [Ghassemieh, 2012] executed in the computer model.

This model describes the constitutive behavior of superelastic SMAs at a constant temperature. The model requires 6 material parameters. The parameters used to define the material model are austenite to martensite starting stress ( $\sigma_{am-s}$ ), austenite to martensite finishing stress ( $\sigma_{am-f}$ ), martensite to austenite starting stress ( $\sigma_{ma-s}$ ), martensite to austenite finishing stress ( $\sigma_{ma-f}$ ), superelastic plateau strain length ( $\epsilon_L$ ), and modulus of elasticity ( $E_A$ ).

The SMA model represents an idealized behavior for SMA material where no strength degradation occurs during cycling and the residual deformation is taken zero at the end of each cycle. A further assumption is that austenite and martensite branches have the same modulus of elasticity ( $\beta = 1$ ), and such simplifications generally have a negligible effect on the response.

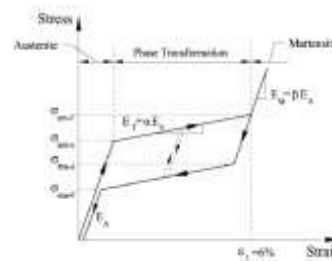


**Figure (5). Stress-strain relationship of the superelastic SMA material. [26]**

The important parameters of the model are listed in Table (1). [24]

**Table (1) Numerical value of the parameters for the modified G-C model.**

Parameters	Nitinol	FNCATB
E N/m <sup>2</sup>	9.8325×10 <sup>10</sup>	5.1 × 10 <sup>10</sup>
E <sub>m</sub> N/m <sup>2</sup>	7.3744×10 <sup>10</sup>	4.1 × 10 <sup>10</sup>
ε <sub>m</sub>	0.08	0.15
ε <sub>l</sub>	0.05	0.095
σ <sub>y</sub> N/m <sup>2</sup>	14.49 × 10 <sup>7</sup>	7.4 × 10 <sup>8</sup>
σ <sub>l</sub> N/m <sup>2</sup>	2.36 × 10 <sup>08</sup>	8.232×10 <sup>8</sup>
n	1	6
α	0.019	0.0187
c	0.001	0.0001
a	900	300
f <sub>t</sub>	0.08	0.95

where:

**E** is the elastic modulus of Austenite,

**E<sub>m</sub>** is the elastic modulus of the pure Martensite

in the wires.

**σ** implies axial stress.

**ε** is the strain

**α** is a constant that control the slope

The coefficients **f** , **c** , **a** are material constants controlling the recovery of the elastic strain during unloading.

## 6. MODELLING OF DAMPERS AND ISOLATORS:

### 6.1. LINEAR MATHEMATICAL MODEL FOR NATURAL RUBBER BEARINGS (NRB) [Michael FEMA 451]- [2],[15]:

Figure 6 shows the modeling for natural rubber bearings and the relationship between the force and the displacement.

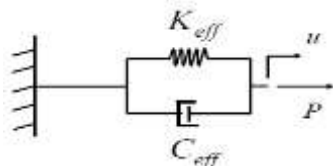


**Figure (6): Mathematical Model for Rubber Bearings (NRB)**

**K<sub>eff</sub>** = Effective stiffness at design Displacement.

**C<sub>eff</sub>** = Effective damping coefficient Associated with design Displacement.

$$P(t) = k_{eff} \cdot U(t) + C_{eff} \cdot \dot{U}(t) \quad (1 - 1)$$

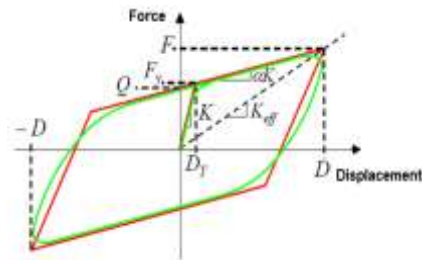


**Figure (7): hysteresis Loop of Rubber Bearings. [1]**

The characteristic of strength (Q) is effectively equal to the yield force (F<sub>y</sub>), of the lead plug. The yield stress of the lead plug is usually taken as being around 10MPa. The effective stiffness (**k<sub>eff</sub>**) of the LRB, at a horizontal displacement (D) being larger than the yield displacement (D<sub>y</sub>) may be defined in terms of the post-elastic stiffness (kd) and the strength characteristic (Q), with the following equation **Figure (7) [1]**:

$$K_2 = \alpha K = (F - F_Y) / (D - D_Y) \quad (1-2)$$

$$K = \frac{F_Y}{D_Y}$$

$$K_{eff} = \frac{F}{D} = \alpha K + \frac{Q}{D} : D \geq D_Y \quad (1 - 3)$$

The energy dissipated for one cycle of sliding, with amplitude (D), **Figure (7)**, can be estimated as:

$$W_D = 4Q(D - D_Y) \quad (1 - 4)$$

$$IFD \gg DY, \text{ Then: } WD \approx 4QD \quad (1 - 5)$$

The effective percentage of critical damping provided by the isolator, **Figure (7)**, can be obtained from:

$$\xi_{eff} = \frac{2Q(D - Dy)}{\pi D(Q + \alpha KD)} \quad (1 - 6)$$

## 6.2. MODELLING OF FLAT

### 6.3. SLIDING BEARINGS:

For Spherical Bearings: [1]

$$F(t) = \frac{W}{R} U(t) + \mu W \dot{U} \quad (1 - 7)$$

Flat Sliding Bearings, **Figure (8-a)** :

$R \rightarrow \infty$  :

$$F(t) = \mu W \sin \dot{U} \quad (1 - 8)$$

Where:

$\mu$ : Coefficient of friction for the sliding.

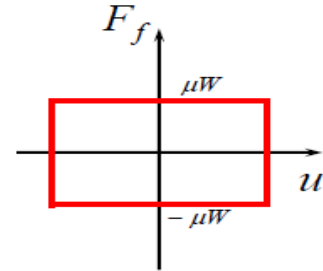
W: Total seismic forces.

$(\dot{U})$  : Continued reference **Figure 8(b)**:

$$\sin(\dot{U}) = \begin{cases} -1 & \dot{U} < 0 \\ +1 & \dot{U} > 0 \\ 0 & \dot{U} = 0 \end{cases}$$



(a)



(b)

**Figure (8): (a) Flat Sliding Bearings, (b) Friction Response. [1]**

- Bearings do not increase natural period of structure; but they limit the shear force transferred into the superstructure.
- Supplemental self-centering mechanism are required to prevent permanent isolation system displacement.

### 6.4. Rotation Friction Dampers (FD):

Modeling of friction damper as spring form (**Plastic Wen link [14], Figure (9)**).

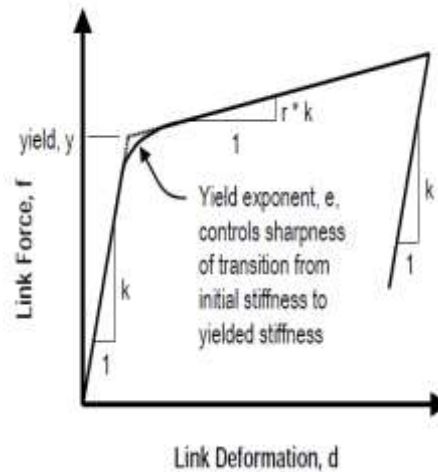


**Figure (9): the power relationship - transmission of the damper (FD)**

The force in the Rotation Friction Dampers (FD) are determined in, **Figure (9)**, by the following equation:



$$F = rkd + (1 - r)yz \quad (1 - 9) \quad [14]$$

Z: hysteretic variable where  $-1 \leq z \leq 1$ , the initial value of z is zero.

F: force,  
d: deformation,  
K: Stiffness,  
y: Yield force,  
r: Yield ratio.

### 6.5. Basic recentering shape memory alloys Damping Devices: [24]

The superelastic stress-strain behavior of SMA wire restrainer is discussed with reference to the plot in **Figure (5)**. The superelastic stress-strain behavior has been characterized by different phenomenological models. Among these, the Graesser- Cozzarelli model which has been widely employed for studying the dynamic behavior of SMA. However, in order to accommodate larger strain at which further hardening like behavior due to Martensite transition occurs, the G-C model is extended by Wilde et al. The modified model is then expressed as:

$$\frac{d\sigma}{dt} = E \left[ \frac{d\varepsilon}{dt} - \left| \frac{d\varepsilon}{dt} \right| \left( \frac{\sigma - \beta}{Y} \right)^n \right] u_I(\varepsilon) E_m \left( \frac{d\varepsilon}{dt} \right) u_{II}(\varepsilon) + \left( 3a_1 \frac{d\varepsilon}{dt} \varepsilon^2 + 2a_2 \text{sign}(\varepsilon) \frac{d\varepsilon}{dt} \varepsilon + a_3 \frac{d\varepsilon}{dt} \right) u_{III}(\varepsilon) \dots \dots \dots (1-10)$$

in this expression,  $\sigma$  refers to axial stress,  $\varepsilon$  is the strain, E is Modulus of elasticity of Austenite,  $E_m$  is the elastic modulus of the pure Martensite in the wires. The variable (t) is the pseudo-time to define the stress/strain rate. The parameters ( $a_1, a_2, a_3$ ) are constants to control the curvature associated with the phase transition. These constants are selected so that the slopes of the function

defined by the last term in Eq. (1-10) at strain levels ( $\varepsilon_1, \varepsilon_m$ ) are consistent with the slopes observed in the experimental force-deformation behavior of the SMA. The smoothness of the loop is ensured by the selection of the slope at strain ( $\varepsilon_2$ ). The functions  $u_I(\varepsilon), u_{II}(\varepsilon), u_{III}(\varepsilon)$  are described as( $\varepsilon$ ):

$$u_I(\varepsilon) = (1 - u_{II}(\varepsilon) - u_{III}(\varepsilon)) \quad (1-11.a)$$

$$u_{II}(\varepsilon) = \begin{cases} 1 & |\varepsilon| \geq \varepsilon_m \\ 0 & \text{otherwise} \end{cases} \dots \dots \dots (1-11.b)$$

$$u_{III}(\varepsilon) = \begin{cases} 1 & \varepsilon \frac{d\varepsilon}{dt} > 0 \text{ and } \varepsilon_1 < |\varepsilon| < \varepsilon_m \\ 0 & \text{otherwise} \end{cases} (1-11.c)$$

The term  $E_m \left( \frac{d\varepsilon}{dt} \right) u_{II}(\varepsilon)$  in Eq. (1-10) describes the martensite elastic behavior, activated as the strain which is higher than  $\varepsilon_m$ , from austenite to martensite the strain at which the transformation is completed. The transition of the slope from  $E_y$  to  $E_m$  is obtained by adding the third/last term in Eq. (1-10), and evaluated during loading and in the strain range  $\varepsilon_1 < \varepsilon < \varepsilon_m$ . The parameter  $\beta$  is the one-dimensional back stress, the evolution of which is described as:

$$\beta = E\alpha \left\{ \varepsilon^{in} f_1 |\varepsilon|^c \text{erf}(\alpha\varepsilon) \left[ H \left( -\varepsilon \frac{d\varepsilon}{dt} \right) \right] \right\} \dots \dots \dots (1-12)$$

$\varepsilon^{in}$  represents the inelastic strain, and it is defined as

$$\varepsilon^{in} = \left\{ \varepsilon - \left( \frac{\sigma}{E} \right) \right\} \dots \dots \dots (1-13)$$

The parameter  $\alpha$  is a constant that controls the slope and is given by

$$\alpha = (E_y / (E - E_y)) \dots \dots \dots (1-14)$$

where  $E_y$  is the slope after yielding, The function erf (.) and H (.) is the unit step function defined as

$$\text{erf}(x) = \frac{2}{\sqrt{\pi}} \int_0^x e^{-t^2} dt \dots\dots\dots (1-15)$$

$$H(x) = \begin{cases} 1 & x \geq 0 \\ 0 & x < 0 \end{cases} \dots\dots\dots (1-16)$$

The coefficients f, c, a t are material constants controlling the recovery of the elastic strain during unloading. At present, the SMA component is in the form of wires, which are subjected to cyclic axial loading, and therefore the restoring force in the restrainer is expressed as

$$FS = A * \sigma \dots\dots\dots (1-17)$$

where A is the total area of the wire restrainer and  $\sigma$  is the axial stress in the bar. The behavior during tension and compression is assumed to be identical in this model.

Superelastic SMA behavior is possible to simulate in finite element software SAP2000 as described. **Figure** (10), by adding two link properties and assign them to two link elements in parallel. A multi-linear plastic link using the Pivot model is used to define the hysteresis loop, and a multi-linear elastic link is used to shift the hysteresis loop away from the origin (see Fig.10.a), input cosine wave excitation, hysteresis curve of the damper is obtained (see Fig.10.b). As can be seen from (Fig.10.b), the shape of hysteresis curve presents flag, which shows that the method can approximately simulate re-centering SMA Damping Devices, which calibrated in [25],

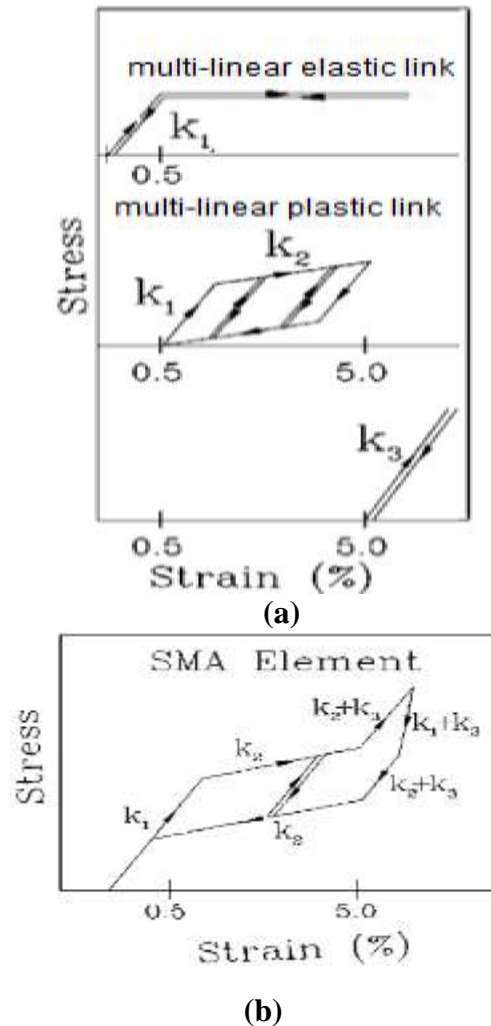


**Figure (10): Schematic diagram of the superelastic SMA, (a)Schematic diagrams of element models, (b)Hysteresis curve of recent ring SMA damper[25]**

**7. ANALYTICAL STUDY:**

Studying the dynamic behavior of Shape memory alloys SMA re-centering damping system, which acts in tension, nonlinear time history analyses were performed, **Figure** (1), El Centro earthquake was selected for Time History analysis to understand the seismic performance of the studied building.

The computational model of the structures was developed using the modeling capability of the software

(sap2000-v22). The building was studied using several heights (eight, twelve, and sixteen stories), to understand the seismic behavior of structure with SMA re-centering damping system. Four analysis methods were used to determine performance of a multi-story building isolated and that was done by using isolation systems (Rubber and Flat Sliding isolators) (FSB+LRB)), and the addition of the dampers and re-centering SMA Damping Devices at the base of the building: Shape memory alloys FNCATB (SMA) (SMA+FSB+LRB) and compared with the performances of the rotation friction dampers (FD+FSB+LRB) and its impact on structure response.

### 7.1. The study cases:

**Figure (11)** shows the studied building by Combination of Rotation Friction Dampers FD, lead rubber bearings LRB and Flat sliders bearings FSB.

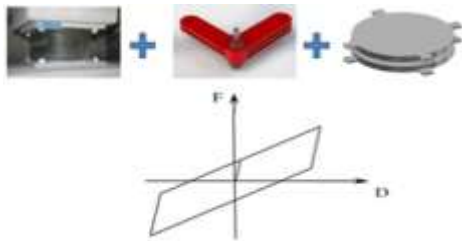


**Figure (11): Response mechanism of combined isolation system (FD+LRB+FSB)**

**Figure (12)** shows the studied building by Combination of recentering Shape memory alloys Damping Devices, rubber bearings and flat sliders bearings.

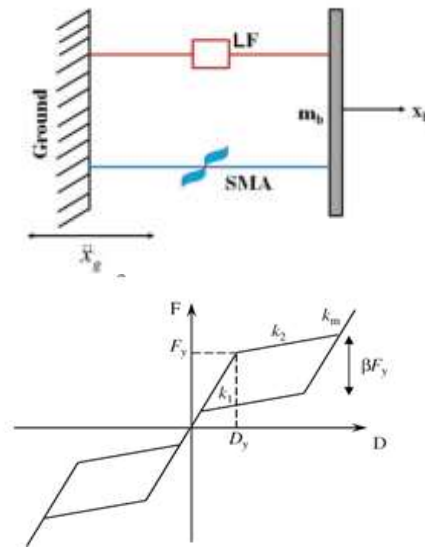
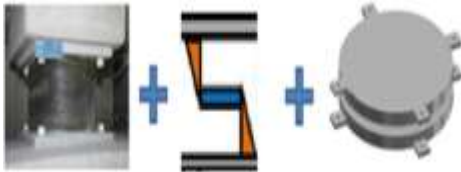


**Figure (12): Schematic view and idealized hysteresis of isolators: (a) LF(LRB+FSB) and (b) Re-SMA.**

**Where:**

$M_b$ : is the mass of the isolator base.

$\ddot{x}_g$ : is the ground acceleration.

LF: LRB+FSB

$x$ : is the relative displacement vector of the superstructure relative to the base mass.

$F_y$ : Yield force

$D_y$ : Yield displacement

$\beta$ : ratio of unloading and loading stress.

$K_1$ : elastic stiffness

$K_2$ : Post-elastic stiffness

$E_m$ : the elastic modulus of the pure Martensite in SMA wires.

#### 7.1.1. PROPERTIES OF MATERIAL AND STRUCTURES USED:

Eight storied tall, bay reinforced concrete was considered in this study. **(Figure (13) and (2))** [11], the story heights are 3m, columns dimensions: 50X50 cm, dimensions of Beams: 70X30

cm, Solid slab thickness 15 cm, loads of coverage: 3 kN / m<sup>2</sup>, live loads: 3 kN / m<sup>2</sup>.

The required material properties like mass, weight density, modulus of elasticity shear modulus and design values of the material used can be modified as per requirements or default values can be adopted Beams and column members have been defined as ‘frame elements’ with the appropriate dimensions and reinforcement. Soil structure interaction was not been considered.

Slabs were defined as area elements having the properties of shell elements with the required thickness.

In our case, the slabs have been modeled as rigid diaphragms and, in this connection, the center of rigidity (mass) and center of gravity of the building are considered the same in order to neglect the effect of torsion.

Properties for Lead Rubber bearing (LRB) used in this study as follows:

Effective horizontal stiffness:  $k_{eff} = 825$  kN / m

Effective Damping:  $C_{eff} = 67.140$  KN. Sec / m Yield strength:  $f_y = 54.43$  KN

Properties for FLAT SLIDING BEARING (FSB) Friction force equal to 10% of dead load:

$$F(t) = \mu W \quad F(t) = 0.10WD,$$

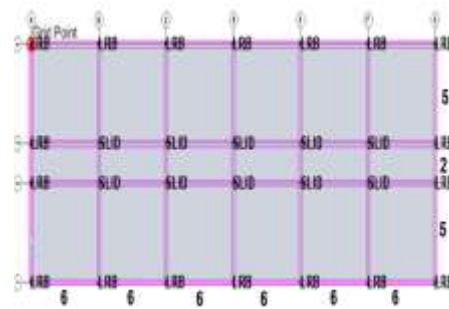
The numerical value of the parameters for FNCATB(SMA), listed in Table (1).

properties for Rotation Friction Dampers **Figure (9)** used in this study as follows:

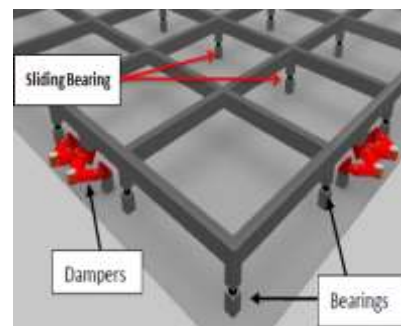
Stiffness,  $k=15000$  kN/m →

$F=150$ kN → Yield force,  $F_y=15$  kN

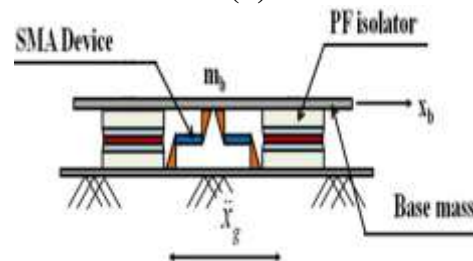
Yield ratio:  $r=0.00001$ , Yield exponent:  $e=20$ .



(a)



(b)



(c)

**Figure (13): (a): Plan View of Symmetrical Building Shown by the distribution of seismic isolators and dampers, (b): The rotation friction dampers at the base of the building (FD), (c): The Shape memory alloys SMA re-centering Damping Devices at the base of the building (SMA).**

## 7.2. Analytical results:

### 7.2.1. Starting analysis with case, eight-storied building, and comparisons:

By analysis results, we found the values of: (Period), (Displacements) **Figure**

(15), (drift) **Figure (16)**, and (Base shear) **Figure (17)**,

The values of Period for the building with height 8 stories, as isolation cases:

- T(Fixed)=0.7 sec
- T(FSB+LRB) =1.9 sec
- T (FD+LRB+ FSB) = 0.9 sec
- T (SMA+LRB+ FSB) = 1.89 sec

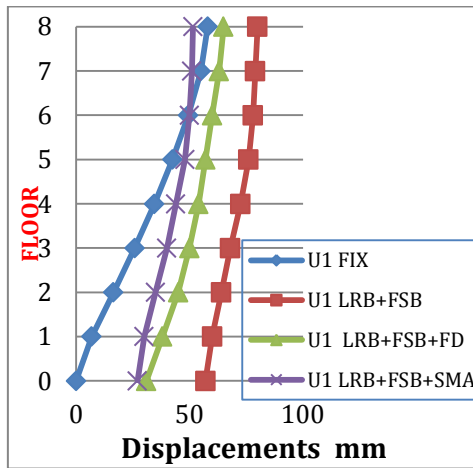


**Figure (15):** Stories displacements of the building with height of 8 stories

The results in **Figure (15)**: show that, the use of (RE-SMA) with isolation systems (FSB+LRB), work to reduces displacements (about 40%), and the use of (FD) with isolation systems (FSB+LRB), work to reduce displacements (about 25%), in comparison with using isolation systems (FSB+LRB).

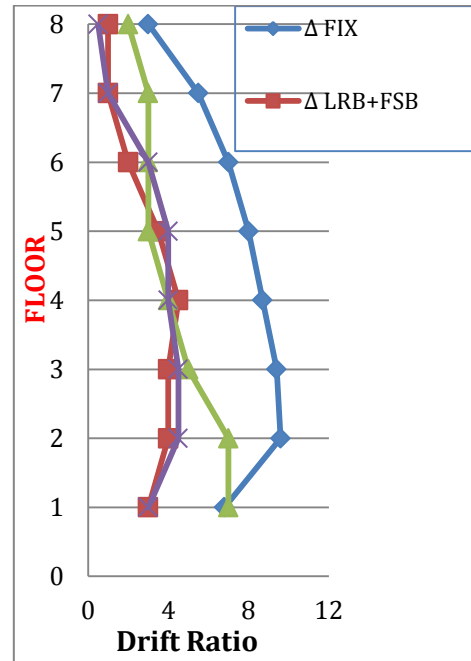


**Figure (16):** Floor drift ratio of the building with height of 8 floors

The results in **Figure (16)**: show that, the use of (RE-SMA) with isolation systems (FSB+LRB), work to increases drifts (about 7%), and use of (FD) with isolation systems (FSB+LRB), work to increase drifts (about 45%), in comparison with using isolation systems (FSB+LRB). This is because the increase in the rigidity of the isolation system brings the building closer to the fixed building.

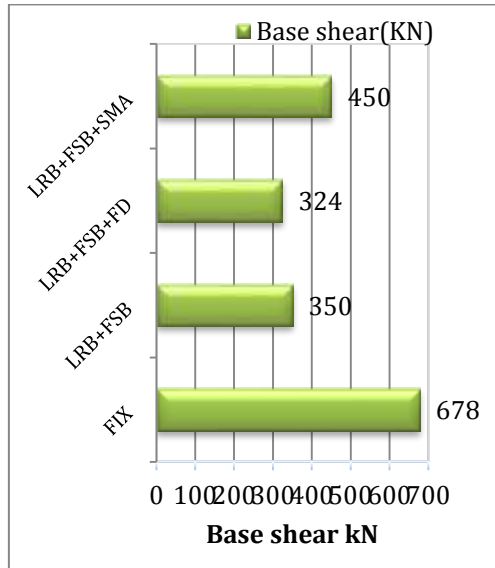


Figure (17): Base shear of the building with height of 8 floors

The results in Figure (17): show that, the use of (RE-SMA) with isolation systems (FSB+LRB), work to increase **Base shear** (about 28%), and use of (FD) with isolation systems (FSB+LRB), work to reduce **Base shear** (about 8%), in comparison with using isolation systems (FSB+LRB).

Therefore the results in Figs.15,16 and 17 show the values of inter-floors drift, displacements and Base shear for eight-floor building with four different isolation cases, (Fix), (FSB+LRB), (FSB+LRB+RE-SMA), (FSB+LRB+FD), and the results show that, the use of recentering SMA Damping Devices (RE-SMA) with isolation systems (FSB+LRB), works well at reducing both drifts (on average 29%), displacements (on average 20%), and increases the Period (from 0.9 to 1.89), but it has a negative effect about Base shear, because it increases it (on average 38%), in comparison with the use of rotation friction dampers (FD) with isolation systems (FSB+LRB).

### 7.2.2. Complete analysis with increasing the floors to 12 and 16, and compares the results:

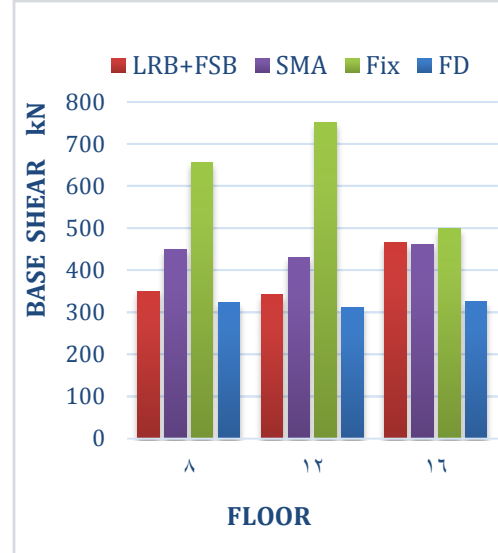


Figure (18): the change in base shear with increasing the height of the building to cases of isolation (LRB, FSB, FD, SMA)

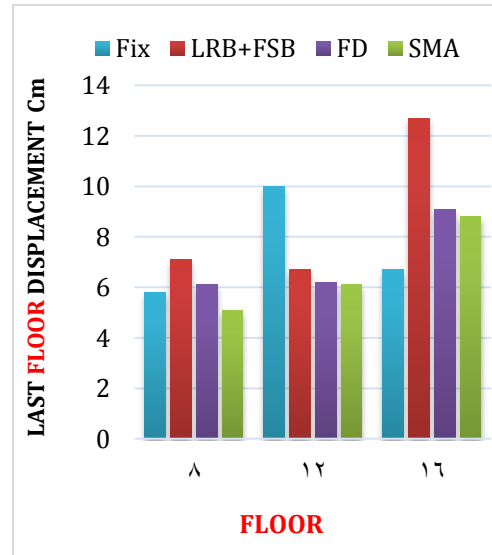


Figure (19): the displacements in the last floor with increasing the height of the building to cases of isolation (Fix, LRB, FSB, FD, SMA)

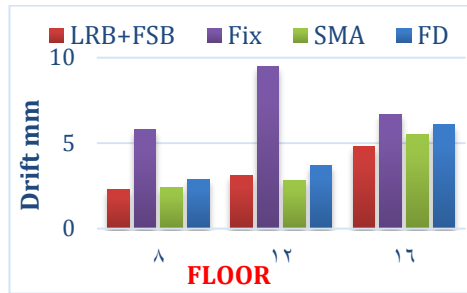


Figure (20): Drift with increasing the height of the building to cases of isolation (Fix, LRB, FSB, FD, SMA)

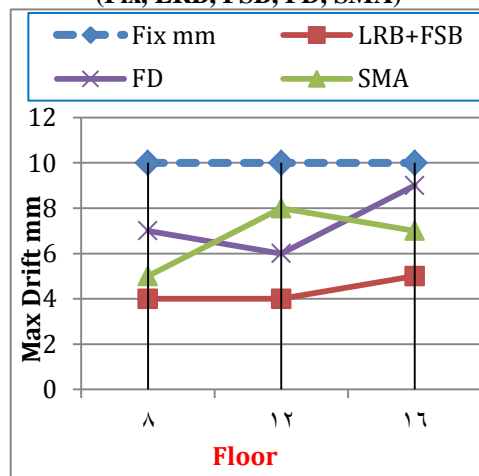


Figure (21): Max Drift with increasing the height of the building to cases of isolation (Fix, LRB, FSB, FD, SMA)

The Figure (18, 19, 20, 21) show the results which indicate effectiveness of the use recentering Shape memory alloys Damping Devices (RE-SMA) in isolation systems (FSB+LRB), and increasing the flexibility of the structure (increase the structure height) for several parameters, Base shear, Displacements in the last floor, Drift and Max Drift Compared with Allowed Drift.

In the 12-floor building, the results show that, the use (RE-SMA) with (FSB+LRB) reduces the inter-floor drift (on average 24%), reduces the displacements in the last floor (on average 2%), increase Base shear (on average 38%

(negative effect)), The Max Drift is less than allowed drift (on average 20%) while the max drift with (FD) less than allowed drift (on average 40%), All these results are in comparison with using (FD) in isolation system (FSB+LRB)

Also, in the 16-floor building, the results show that, using (RE-SMA) with (FSB+LRB) reduces the inter-floor drift (on average 10%), reduces the displacements in the last floor (on average 3%), increases Base shear (on average 40% (negative effect)), the Max Drift is less than allowed drift (on average 30%) while the max drift with (FD) less than allowed drift (on average 10%), All these results are in comparison with using (FD) in isolation system (FSB+LRB).

## 8. RESULTS:

- 1- In this paper, the efficiency of superelastic behavior of shape-memory alloys (SMA) is verified in seismic response reduction of structures, so shape-memory alloys could be effectively utilized for seismic design of structures with the purpose of protecting building structures against earthquakes corresponding to several seismic hazard levels.
- 2- Using recentering Shape memory alloys Damping Devices (RE-SMAs) with hybrid isolation system (LRB + FSB) at the base of the structure has a significant impact in improving the performance of isolated structure comparing with the use of rotation friction dampers (FD) with (LRB + FSB), in terms of reducing Displacements (on average 7%), Drift (on average 16%) with increasing height of structure from 8

to 16 floors, but it has a negative impact on the Base shear which led to an increase in the Base shear (on average 30%), because the damping capacity to (RE-SMAs) is less than the (FD), but it is compensated by the re-centering.

- 3- Although the results show that promise for implementing the superelastic behavior of shape-memory alloys (RE-SMAs) in seismic isolation, still further works are necessary to confirm the numerical simulations and the analytical results experimentally.
- 4- The results of displacement show that the displacements are increased (on average 17%) with the period and with the floor-height from 8 to 16 floors in the base isolated building by (LRB + FSB) comparing with fixing building because the effectiveness of the isolation system decreases for high structures.
- 5- The case of base isolation system (LRB + FSB) with additional FD, is more effective for a sixteen-floor-height building, and the case of base isolation system (LRB+FSB) with additional Re-SMAs, is more effective for an eight-floor-height building.
- 6- The effectiveness of hybrid isolation system (LRB + FSB) in reducing the base shear and drift of the structure isolated decreases with increasing the flexibility of structure.
- 7- Therefore, the results imply that, in the event of earthquakes, due to the excellent super-elasticity of recentering Shape memory alloys Damping Devices (RE-SMAs), the replacement or refurbishment of the isolation system will not be necessary.

## 6. RECOMMENDATION:

Although the results suggest promise for implementing the superplastic behavior of shape-memory alloys (SMA) in seismic isolation, further works are necessary to confirm the numerical simulations and the analytical results experimentally.

## 7. REFERENCES:

- [1] Michael D. and Symans, Design Examples Seismic Isolation, Instructional Material Complementing FEMA 451.
- [2] Kelly and Trever, Base Isolation of Structure, Design Guideline Holmes Consulting Group, 2001.
- [3] Naeim, F. and Kelly, J., Design of seismic isolated structures, Wiley, New York, 1996.
- [4] Jangid, R.S., Optimum friction pendulum system for near-fault motions, Engineering Structures, 2004.
- [5] Leif, O., Imad, H., Mualla and Yuuichi, Seismic isolation with a new friction-viscoelastic damping system, 13th World Conference on Earthquake Engineering, Vancouver, B.C., Canada, August 1-6, 2004.
- [6] Earthquake Protection Systems, Technical Characteristics of Friction Pendulum Bearings, Vallejo, California, 2003.
- [7] Tsai C.S., Chiang T.C. and Chen B.J., Seismic behavior of MFPS isolated structure, JC Chen, editor. Seismic engineering, ASME, 2003, PP. 73-9.
- [8] Fenz D.M. and Constantine M.C., Behavior of the double concave Friction Pendulum bearing. Submitted for review and possible publication in Earthquake Engineering and Structural Dynamics, 2005.
- [9] Troy A., Morgan, Stephen A. and Mahin, The Use of Base Isolation Systems to Achieve Complex Seismic Performance Objectives, Pacific Earthquake Engineering Research Center College of Engineering University of California, Berkeley, 2011.
- [10] Toyooka A., Himeno T., Hishijima Y., Iemura H. and Mualla I., Verification Tests of Dynamic Behavior of the Novel



- Friction- Based Rotational Damper Using Shaking Table, The 14 The World Conference on Earthquake Engineering, Beijing, China, October 12-17, 2008.
- [11] Tracy Thaeer, The behavior of Seismically Isolated Buildings Using Rubber Bearing, Master, the Higher Institute of Seismic Studies and Research, University of Damascus, 2011.
- [12] Shirule P.A., Jagtap L.P., Sonawane K.R., Patil T.D., Jadwanir N. and Sonar S.K., Time History Analysis of Base Isolated Multi-Storied Building, International Journal of Earth Sciences and Engineering, ISSN 0974-5904, Vol. 05, No. 04, 2012, PP. 809-816.
- [13] Wang and Yen-Po, Fundamentals of Seismic Base Isolation, International Training Programs for Seismic Design of Building Structures Hosted by National Center for Research on Earthquake Engineering Sponsored by Department of International Programs, National Science Council, 2009.
- [14] SAP2000, Software Verification.
- [15] Andrade L. and worth J.T., Seismic Protection of Structures with Modern Base Isolation Technologies, Concrete Solutions, 2009. pp. 7a-3.
- [16] Structural Protection Systems, MAURER Seismic Isolation Systems with Lead Rubber Bearings (LRB), SPS/02.05. 2003. PP. 1-9
- [17] Nagarajaiah S. and Sun X., Base-isolated FCC building: Impact response in Northridge earthquake, J. Struct. Eng. Vol. 127, Issue 9, 2001, pp. 1063–1075.
- [18] Kelly J.M., The role of damping in seismic isolation. Earthq. Eng. Struct. Dyn., Vol. 28, 1999, pp. 3–20.
- [19] Nagarajaiah, S. and Sun X., Base-isolated FCC building: Impact response in Northridge earthquake. J. Struct. Eng. Vol. 127, 2001, pp. 1063–1075.
- [20] Dolce M., Cardone D. and Marnetto R., Implementation and Testing of Passive Control Devices Based on Shape Memory Alloys, Earthquake Engineering and Structural Dynamics, Vol. 29, Issue 7, 2000, pp. 945-968.
- [21] Ma H. and Cho C., Materials Science and Engineering A., Vol. 473, 2008, pp. 290.
- [22] Ponzo, F.C., Nigro, D., Dolce M., Cardone, D. and Cacosso A., Comparison of different seismic isolation systems through shaking table tests on a steel structure, In Proceedings of the 3<sup>rd</sup> World Conference on Structural Control, Como, Italy, 2002.
- [23] Qiu C. and Zhu S., Characterization of cyclic properties of superplastic monocrystalline Cu-Al-Be SMA wires.
- [24] Sutanu Bhowmick & Sudib Kumar Mishra, "Ferrous SMA (FNCATB) based Superelastic Friction Bearing Isolator (S-FBI) subjected to pulse type ground motions" Soil Dynamics and Earthquake Engineering 100 (2017) 34–48.
- [25] Bhowmick S. and Mishra S.K., Ferrous SMA (FNCATB) based Superelastic Friction Bearing Isolator (S-FBI) subjected to pulse type ground motions, Soil Dynamics and Earthquake Engineering, Vol. 100, 2017, PP. 34–48.
- [26] Ghassemieh M., Bahaari M., Ghodrati S. and Nojoumi S., Improvement of Concrete Shear Wall Structures by Smart Materials, Open Journal of Civil Engineering, Vol. 2, 2012, PP. 87-95.
- [27] Andrawes, B. and DesRoches R., Unseating prevention for multiple frame bridges using superelastic devices. Smart Mater. Struct., Vol. 14, No. 3, 2005, S60–S67